VIII International Conference on Particle-Based Methods
PARTICLES 2023
U. Perego, M. Cremonesi, A. Franci (Eds)

NUMERICAL SIMULATION OF A LABORATORY-SCALE FREE FALL CONE PENETROMETER TEST IN MARINE CLAY WITH THE MATERIAL POINT METHOD

D. MOHAPATRA[1], M. SARESMA[2], J. VIRTASALO[2]AND W. SOŁOWSKI [1]

[1] Department of Civil Engineering
Aalto University
Rakentajanaukio 4, 02150 Espoo, Finland
email: debasis.mohapatra@aalto.fi, www.aalto.fi

[2] Geological Survey of Finland
Vuorimiehentie 5, 02150 Espoo, Finland
email: gtk@gtk.fi, www.gtk.fi

Abstract. This paper shows a numerical replication of a laboratory-scale free fall cone penetrometer test of marine clay. The numerical simulation involves large deformations and considers the destructuration of clay, strain rate effects, and non-linear material behaviour. The numerical simulation well replicates the laboratory experiment captured on a high-speed camera. The penetration process is replicated accurately in time, and the depth of the penetration corresponds to that obtained in an experiment. The simulation results indicate that the numerical framework implemented in Uintah software, consisting of an advanced soil model and the Generalized Interpolation Material Point Method, is well-suited for replication of the dynamic penetration process in soft and sensitive marine clay.

Keywords: Free fall cone penetrometer test, Generalized Interpolation Material Point Method, Contact Problems, Strain rate, Destructuration.

1 INTRODUCTION

The free fall cone penetrometer tests (FF-CPT) are simple, rapid, and cost-effective tests that can be used in seabed characterization [1]. However, there are still uncertainties in the interpretation of the test data and its correlation with the soil properties. The currently used correlations are empirical [2–4], mainly because of the complexities associated with the numerical simulation of the dynamic penetration process. Therefore, the development of reliable numerical models that can replicate the dynamic penetration process may lead to more accurate correlations and data interpretation, improving the accuracy of the soil properties obtained with FF-CPT.

In recent years, many experimental [2,3,5] and numerical studies [6,7] investigated the cone penetration mechanism associated with the FF-CPT. The studies point out that the uncertainties in FF-CPT data interpretation could be due to the wide range of strain rates associated with the test. However, the determination of the strain rate effect on the shear strength of soil is quite complicated due to its possible dependency on soil properties, cone penetrometer parameters

(e.g., geometry, density), and impact velocity. Further, the marine clays are also sensitive, and their undrained shear strength reduces during the cone penetration process due to the destructuration of clay. Not considering the effects of strain rate and destructuration on clay will significantly influence the accuracy of the numerical simulation.

In the present study, we replicate a laboratory-scale free fall cone penetrometer test results with the Generalized Interpolation Material Point Method simulation. The numerical simulation results that consider the effect of strain rate and destructuration of clay well replicate the dynamic penetration process of the cone penetrometer dropped from a height.

2 LABORATORY-SCALE FREE FALL CONE PENETROMETER TEST SETUP AND TEST PROCEDURE

The study uses soft and sensitive marine clay samples collected from the south of Kytö island in the Gulf of Finland, north of the Baltic Sea. The clay parameters are summarized in Table 2. To understand the dynamic cone penetration mechanism associated with the FF-CPT, a series of well-controlled laboratory tests are conducted using a model cone penetrometer. The model cone penetrometer, shown in Figure 1b, has a similar geometry to the Graviprobe 2.0 (©dotOcean), which is often used in FF-CPT. The cone penetrometer is a steel cone of 5 mm diameter and 60 mm length with 60° apex angle (Figure 1c). The model cone penetrometer is attached to a steel shaft, as shown in Figure 1b. Some additional steel weights are attached at the bottom of the shaft to make its weight 60 g. Figure 1a shows the laboratory free fall cone setup. The model cone penetrometer, along with the shaft, is attached to a frame, from where it can be released from different heights into the soil sample. The dial gauge is attached to the frame to measure the final penetration depth (Figure 1a).

The present test program involves five test series, including 10 fall cone tests and 15 laboratory-scale free fall cone penetrometer tests. The fall cone tests are carried out to obtain the theoretical value of the undrained shear strength (s_u) of clay by using two different cones, namely, (i) a 30° 100g cone and (ii) a 60° 60g cone. The value of undrained shear strength of clay is found to be 7.4 kPa for a 30°cone and 6.96 kPa for a 60° cone [8]. The laboratory-scale FF-CPTs are conducted by releasing the cone penetrometer from different heights: 0 mm, 10 mm, and 20 mm. This paper focuses on a replication of a single test from the testing program, where the cone penetrometer is dropped into the soil surface from a height of 10 mm. The free fall cone penetrometer tests are carried out at five different points on the sample surface (labeled FFP-1-1 to FFP-1-5). A minimum separation of 2.5 times the cone diameter is maintained between the two tests to minimize interference and any boundary effects. This separation is believed to be sufficient, as numerical simulation (Figure 7) shows that most of the radial deformations are concentrated within 2 cone diameters. The final penetration depths (d_f) associated with these tests are reported in Table 1. The displacement, velocity, and acceleration profiles associated with the cone indentation process in the free fall cone experiments are obtained by using the MATLAB image processing technique described in [9]. Figures 4-6 show that the displacement, velocity, and acceleration profiles of the cone associated with different points in the experiments are similar. Figure 4 shows that the cone hits the ground soil surface after approximately 0.05 sec.In all cases, After the cone penetrometer hits the ground, the process of cone penetration into soil takes less than 0.05 seconds. Figure 5 shows that The cone penetrometer hits the soil surface at a velocity of approximately 0.43 m/s. The acceleration

profiles in Figure 6 indicate that the acceleration at the very beginning of the experiment (up to approximately 0.02) was lower than the gravitational acceleration. This slowdown may be caused by friction mobilized in the cone shaft during the cone release for free fall. After that, the cone penetrometer moves with gravitational acceleration untill it hits the soil surface.

Table 1: Final penetration depth of cone (d_f) from different experiments

Tests	**Final penetration depth, d_f (mm)**
FFP-1-1	11.1
FFP-1-2	10.1
FFP-1-3	11.6
FFP-1-4	11.0
FFP-1-5	10.6
Numerical Analysis	9.6

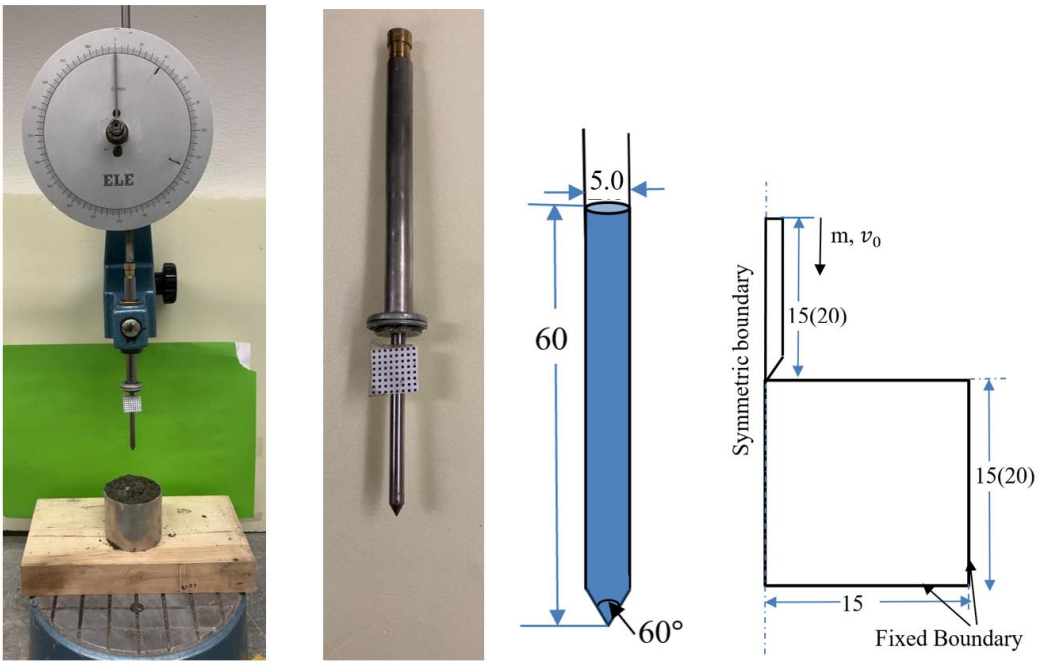

Figure 1: (a) Model test set-up; (b) Model cone penetrometer; (c) Cone penetrometer geometry; (d) Numerical model of FF-CPT. Unit: mm

3 NUMERICAL MODELLING USING GIMP

3.1 Description of the Generalized interpolation material point method (GIMP)

The material point method (MPM) is a particle-based method well-suited to solve dynamic large deformation problems [10]. However, the original MPM has lots of numerical instability issues when

particles pass through element boundaries. The generalized material point method (GIMP) is an updated version of the material point method that uses a particle characteristics function to reduce cell-crossing errors [11]. This paper uses GIMP as encoded in Uintah software (http://uintah.utah.edu/) for simulations of the fall cone test.

3.2 The material constitutive model

The entire process of the laboratory FF-CPT is very short (less than 0.1 sec). Therefore, for fully saturated clay, there will be no volume change (undrained conditions). Hence, the shear strength will be related to the undrained shear strength. Among others, [12–14] show that the undrained shear strength of clay depends on the shear strain rate and destructuration of clay. Therefore, in the simulations, we use the Tresca material model extended to consider the effect of strain rate and destructuration on undrained shear strength as mentioned in [12,15]. The undrained shear strength of clay is expressed as a function of strain rate ($\delta\gamma$), accumulated shear strain (ξ), and sensitivity (S_t) as:

$$s_u(\delta\gamma, \xi, S_t) = s_{u,ref}\left(\frac{\delta\gamma}{\delta\gamma_{ref}}\right)^{\beta}\left[\frac{1}{S_t} + \left(1 - \frac{1}{S_t}\right)e^{\frac{-3\xi}{\xi_{95}}}\right] \tag{2}$$

where $s_{u,ref}$ is reference shear strain at reference strain rate ($\delta\gamma_{ref}$), β is the strain rate parameter associated with the power law, and ξ_{95} is the accumulated shear strains required to obtain 95% reduction of the shear strength. For small deformations, the dynamic undrained shear modulus also depends on the shear strain rate and can be estimated as

$$G_u(\delta\gamma) = G_{u,ref}\left(\frac{\delta\gamma}{\delta\gamma_{ref}}\right)^{\beta} \tag{3}$$

3.3 Numerical model of FF-CPT and selection of material parameters

The GIMP simulation of the laboratory FF-CPT assumes the axisymmetric condition of the fall cone experiment to avoid the computational cost associated with a 3D MPM simulation. Figure 2d shows the numerical model and associated boundary conditions. The analysis uses the average of soil impact velocities obtained from the experiments as the initial velocity of the cone penetrometer. The lateral and vertical spread of the soil domain is decided based on a few trial analyses, so that the boundaries will not influence the outcome of the numerical simulation. The GIMP simulation uses the elastic material model to model the steel free fall cone penetrometer. The density of the fall cone material in the simulation is such that the simulated cone weight is 60 g, corresponding to the experiment.

The experimentally measured value of sensitivity (s_t) of the clay sample is approximately 10 and the density of the material is 15 kN/m^3. As mentioned in Section 2, the reference undrained shear strength ($s_{u,ref}$) of clay is set to be 7.2 kPa based on the laboratory fall cone test. The reference elastic shear modulus is set to be 167 times the undrained reference shear strength value, as mentioned in [6]. The undrained Poisson's ratio is set equal to 0.499 to enforce the undrained loading condition. The range of strain rates in a standard fall cone test is approximately 1 to 10 s^{-1} [16,17]. As the duration of the laboratory FF-CPT is shorter than the

standard fall cone test, the associated range of strain rate is supposed to be higher. The value of the reference shear strain is assumed as 0.5 s^{-1}. As the tests are carried out on a similar type of soil as that used in [9], The value of β and ξ_{95} is set to be 0.08 and 10 s^{-1}, respectively. The simulations assume frictional contact with a friction coefficient (μ) developed by [18]. The friction coefficient between cohesive soil and steel lies between 0.5-0.65 [19]. A series of numerical studies have been conducted to examine the influence of the friction coefficient on final cone penetration depth by varying the friction coefficient (μ) from 0 to 1. Figure 2 demonstrates that friction coefficients greater than 0.6 do not significantly change the penetration depth. In the present analysis, we have selected the friction coefficient (μ = 0.65) to prevent sliding between the cone and the clay. Table 2 summarizes the various model parameters considered in the study.

Table 2. Material parameters for numerical simulation

$s_{u,ref}$ (kPa)	$\delta\gamma_{ref}$ (s^{-1})	β	$G_{u,ref}$ (kPa)	υ_u	S_t	ξ_{95} (s^{-1})	ρ (kN/m^3)	μ
7.2	0.5	0.08	$167s_{u,ref}$	0.495	10	10	15	0.65

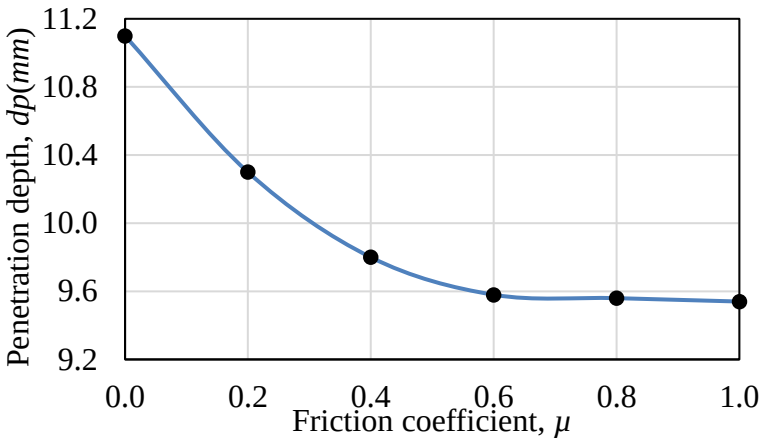

Figure 2. Influence of friction coefficient on the penetration depth of the fall cone penetrometer

3 NUMERICAL REPLICATION OF FREE FALL CONE PENETROMETER TESTS

The grid density in GIMP plays a crucial role in the accurate simulation of the dynamic penetration process [9,20]. To investigate how the grid density impacts the simulation results, the analysis discretizes the problem domain in Figure 1d by using a structured mesh of square sizes (h× h) where h = 1, 0.5, 0.25, and 0.125 mm, each time with 4 material points in the cell. These correspond to 1028, 4114, 16455, and 65820 material points in the simulation,

respectively. Figure 3 demonstrates that with an increase in the number of grid cells, the numerical value of the final penetration depth of the fall cone penetrometer increases and approaches the experimental value of penetration depth. The final penetration depth does not change significantly for h <0.125 mm. Therefore, the present analysis uses h = 0.125 mm for the numerical simulation. The accuracy of numerical simulations can be further improved by increasing the grid density.

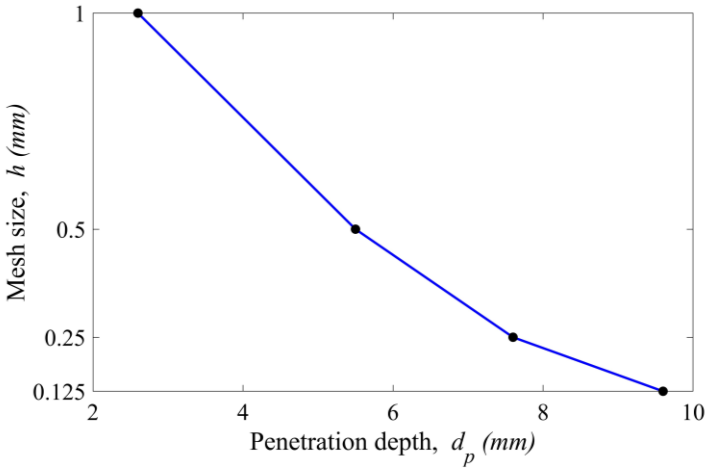

Figure 3. Influence of spatial discretization on the penetration depth of the fall cone penetrometer

The numerical simulation uses grid size h = 0.125 mm and the material parameter as given in Table 2. The cone penetrometer is assigned with an initial velocity of 0.43 m/s based on the value of impact velocity obtained from the experiments. Table 1 shows that the numerical value of the final penetration depth (9.6 mm) is quite close to the average penetration depth obtained from the experiments (10.6 mm). Figures 4, 5, and 6 compare the development of displacement, velocity, and acceleration of the cone pentrometer over time between the experiments and the numerical simulation. Figures 4-6 demonstrate that the numerical and experimental profiles of displacement, velocity, and acceleration associated with the cone penetration process match quite well. Both the numerical and experimental results show that after hitting the soil surface, the cone penetrometer takes around 0.05 seconds to come to a standstill position. The rebound of the cone observed in experiments is quite well simulated numerically. Figure 5 demonstrates that the numerical model predicts the maximum velocity to be approximately 0.46 m/s, which is close to the average maximum velocity from the experiment (0.45 m/s). Figure 6 shows that the numerical cone acceleration oscillates at the completion of the penetration process, with the amplitude of these oscillations decreasing gradually over time. As GIMP is a completely explicit approach that takes into account dynamic forces, the oscillations are presumably the result of the assumed elastic behaviour of the material in the Tresca model at stresses below yield. The small rebounds observed in some of the experiments are well replicated in the numerical simulations. Figure 7 shows the displacement contours associated with the FF-CPT. Figure 7 further shows that the soil surrounding the cone moves in an upward direction with the penetration of the cone. That creates a heave at the soil surface. Figure 7 demonstrates that the radial deformations are concentrated within 10 mm (2 times the diameter of the cone

penetrometer) from the centre of the cone. The experiments should be conducted with a minimum spacing of 2 times the cone diameter to avoid overlapping of distorted zones.

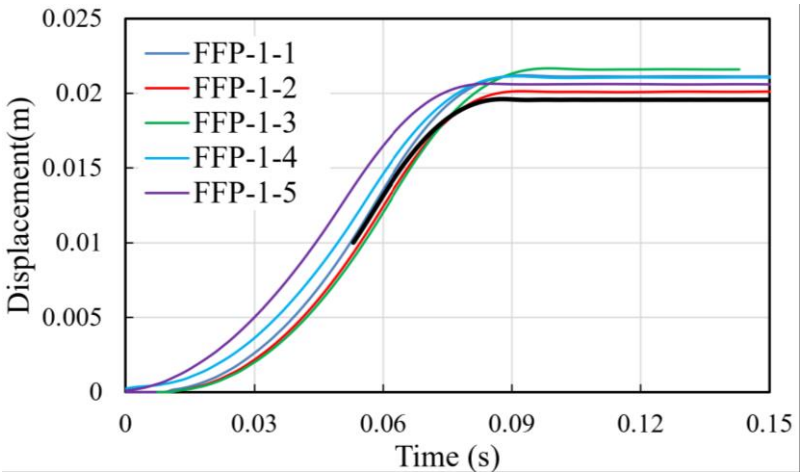

Figure 4: Variation of the Cone penetrometer displacement vs. time

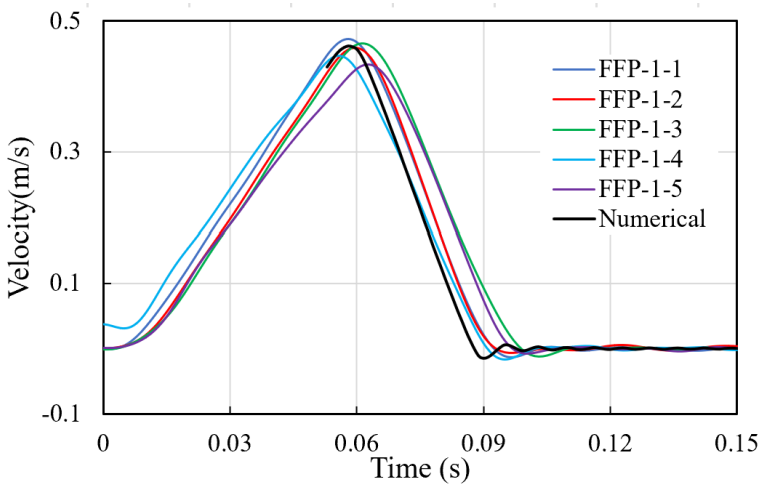

Figure 5: Variation of the Cone penetrometer velocity vs. time

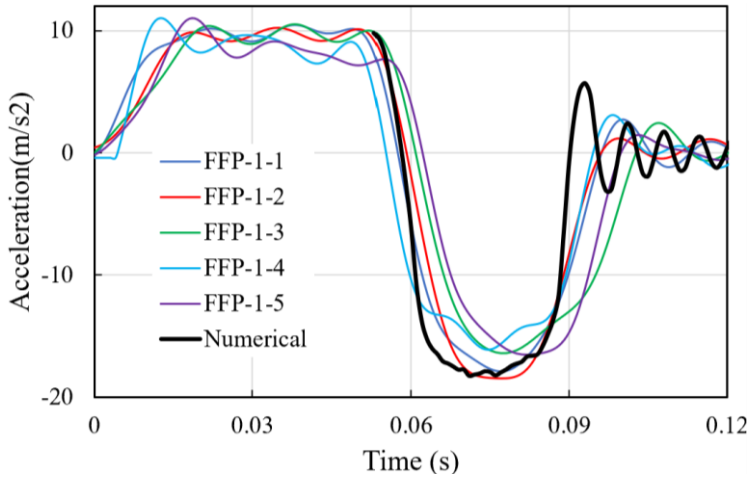

Figure 6: Variation of the Cone penetrometer acceleration vs. time

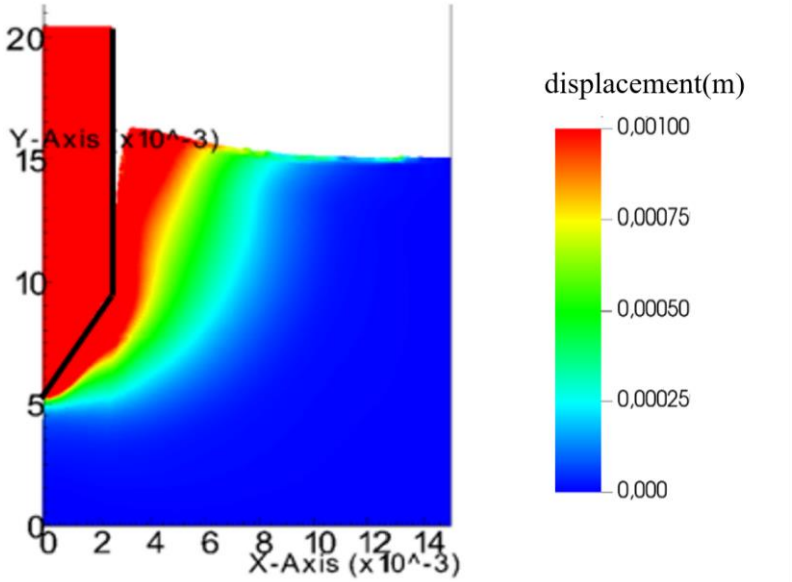

Figure 7: The displacement contours of FF-CPT for different drop heights at the end of cone penetration process

5 CONCLUSIONS

This paper shows a complete numerical simulation of a laboratory-scale free fall cone penetrometer test on marine clay by using the generalized interpolation material point method (GIMP). The theoretical value of the undrained shear strength of the clay obtained from the fall cone test is used for the numerical simulation. An extended Tresca material model is used to consider the effect of strain rate and strain softening due to the destructuration of clay associated with the dynamic cone penetration process. The simulation uses the same material parameters as those used for the numerical replication of the fall cone test in [9]. The experimental results are well replicated by the numerical simulation, with an excellent agreement of the

displacement, velocity, and acceleration profiles of the cone during the penetration process. The results show that the numerical framework used in this work can capture the dynamic penetration mechanism associated with soft and sensitiveclays. The study results give some assurance that the present numerical framework can be used for similar replication in large-scale simulations, such as the in-situ FF-CPT, the installation of dynamic torpedo anchors, and the installation of driven piles. Further, the numerical simulation shows that the cone penetration process during this test influences a surrounding soil zone of two times the cone diameter. Therefore, a minimum separation of two times the cone diameter should be maintained between two adjacent tests to minimize the interference and boundary effect.

6 ACKNOWLEDGEMENTS

This research is part of the Geomeasure project, funded by the Academy of Finland (grant number 347602).

REFERENCES

[1] Stark, N., Hay, A.E. and Trowse, G. Cost-effective geotechnical and sedimentological early site assessment for ocean renewable energies. *2014 Oceans - St John's, NL, Canada* (2014): pp. 1-8.

[2] Chow, S.H. and Airey, D.W. Soil strength characterisation using free-falling penetrometers. *Geotechnique* (2013) **63**:1131–1143.

[3] Chow, S.H., O'Loughlin, C.D., White, D.J. and Randolph, M.F. An extended interpretation of the free-fall piezocone test in clay. *Geotechnique* (2017) **67**:1090–1103.

[4] Bezuijen, A., Den Hamer, D.A., Vincke, L. and Geirnaert, K. Free fall cone tests in kaolin clay. *Physical Modelling in Geotechnics* (2018) **1**:285–291.

[5] Chow, S.H., Asce, A.M. and Airey, D.W. Free-Falling Penetrometers: A Laboratory Investigation in Clay. *Journal of Geotechnical and Geoenvironmental Engineering* (2014)**140**:201–214.

[6] Moavenian, M.H., Nazem, M., Carter, J.P. and Randolph, M.F. Numerical analysis of penetrometers free-falling into soil with shear strength increasing linearly with depth. *Comput. Geotech*. (2016) **72**:57–66.

[7] Zambrano-Cruzatty, L. and Yerro, A. Numerical simulation of a free fall penetrometer deployment using the material point method. *Soils and Foundations* (2020) **60**:668–682.

[8] Koumoto, T. and Houlsby, G.T. Theory and practice of the fall cone test. *Geotechnique* (2015) **51**:701–712.

[9] Mohapatra, D., Li, Z., Saresma, M., Virtasalo, J. and Solowski, W. Replication of fall cone test on marine clay with a Generalized Interpolation Material Point Method simulation. In: Zdravkovic L KSTDTA, editor. *10th European Conference on Numerical Methods in Geotechnical Engineering* (2023). pp.1–7.

[10] Sulsky, D, Zhou, S.J. and Schreyer, H.L. Application of a particle-in-cell method to solid mechanics. *Comput. Phys. Commun.* (1995) **87**:236–252.

[11] Bardenhagen, S.G. and Kober, E.M. The Generalized Interpolation Material Point Method. *Computer Modeling in Engineering and Sciences* (1970) **5**:477–496.

[12] Einav, I. and Randolph, M. Effect of strain rate on mobilised strength and thickness of curved shear bands. *Geotechnique* (2006) **56**:501–504.

[13] Jeong, S.W., Leroueil, S. and Locat, J. Applicability of power law for describing the rheology of soils of different origins and characteristics. *Canadian Geotechnical Journal* (2009) **46**:1011–1023.
[14] Boukpeti, N., White, D.J., Randolph, M.F. and Low, H.E. Strength of fine-grained soils at the solid-fluid transition. *Geotechnique* (2012) **62**:213–226.
[15] Tran, Q.A. and Sołowski, W. Generalized Interpolation Material Point Method modelling of large deformation problems including strain-rate effects – Application to penetration and progressive failure problems. Comput. Geotech. (2019) **106**:249–265.
[16] Koumoto, T. and Houlsby, G.T. Theory and practice of the fall cone test. *Géotechnique* (2001) **51**:701–712.
[17] Boukpeti, N., White, D.J., Randolph, M.F. and Low, H.E. Strength of fine-grained soils at the solid-fluid transition. *Géotechnique* (2012) **62**:213–226.
[18] Bardenhagen, S.G., Guilkey, J.E., Roessig, K.M., Brackbill, J.U., Witzel, W.M. and Foster, J.C. An Improved Contact Algorithm for the Material Point Method and Application to Stress Propagation in Granular Material. *CMES* (2001) **2**:509–522.
[19] Tsubakihara, Y., Kishida, H. and Nishiyama, T. Friction between Cohesive Soils and Steel. *Soils and Foundations* (1993) **33**:145–156.
[20] Tran, Q.A. and Sołowski, W. Generalized Interpolation Material Point Method modelling of large deformation problems including strain-rate effects – Application to penetration and progressive failure problems. *Comput. Geotech.* (2019) **106**:249–265.